PROCEEDINGS OF SCIENCE

Scaling and low energy constants in lattice QCD with $N_f = 2$ maximally twisted Wilson quarks

Petros Dimopoulos, Roberto Frezzotti* **and Gregorio Herdoiza***
Univ. and INFN of Rome Tor Vergata, Via della Ricerca Scientifica 1, I-00133, Rome, Italy
E-mail: {dimopoulos,frezzotti,herdoiza}@roma2.infn.it

Carsten Urbach
Theoretical Physics Division, Dept. of Mathematical Sciences, University of Liverpool
Liverpool L69 7ZL, UK
E-mail: carsten.urbach@physik.hu-berlin.de

Urs Wenger
Institute for Theoretical Physics, ETH Zürich, CH-8093 Zürich, Switzerland
E-mail: wenger@itp.phys.ethz.ch

for the ETM Collaboration

We report on the scaling of basic hadronic observables in lattice QCD with $N_f = 2$ maximally twisted Wilson dynamical quarks. We give preliminary results for some of the Gasser–Leutwyler low energy constants, the chiral condensate and the average mass of *u* and *d* quarks.

The XXV International Symposium on Lattice Field Theory
July 30 - August 4 2007
Regensburg, Germany

*Speaker.

PoS(LATTICE 2007)102

1. Introduction and setup

In this contribution we report on the scaling of basic hadronic observables and present preliminary results for some of the Gasser–Leutwyler low energy constants in lattice QCD with $N_f = 2$ dynamical quarks. We choose the lattice formulation with tree-level improved gauge action and maximally twisted Wilson quarks [1], which can be efficiently studied by means of state-of-the-art simulation algorithms, such as the one we adopted [2], and leads to physical observables free of O(a) cutoff effects [3]. In this way it is possible to study the theory with pion masses down to about 300 MeV, three different lattice resolutions and spatial lattice sizes of 2–3 fm. The main parameters of the simulations employed for the present analysis are summarized in table 1 of Ref. [4]. For all ensembles we have $m_{PS}L \geq 3$, with the lowest values (namely 3.0, 3.3, 3.3 and 3.5) being obtained in the ensembles C6, B1, C1 and C5, respectively. For details about our lattice setup, the evaluation of quark propagators and any undefined notations we refer to Refs. [1, 4].

1.1 Tuning to maximal twist

The values of κ in table 1 of Ref. [4] result from implementing maximal twist as discussed here. The formal definition of maximal twist for Wilson quarks reads: $m_R = 0$ and $\mu_R = O(a^0)$ for all lattice spacings a as $a \to 0$, with renormalized mass parameters

$$\mu_R = Z_\mu \mu = Z_P^{-1} \mu \,, \qquad m_R = Z_{S^0}^{-1}(m_0 - m_{crit}) = Z_A Z_P^{-1} m_{PCAC} \,. \tag{1.1}$$

At the non-perturbative level any legitimate estimate of the critical mass, m_{crit}, is affected by terms of $O(a\Lambda_{QCD}^2)$ and $O(a\mu\Lambda_{QCD})$, which however do not invalidate the definition of maximal twist. Following Refs. [5, 6], for each β (and μ) one can define maximal twist by demanding [1]

$$am_{PCAC}(\beta,\mu) \equiv \frac{a^4 \sum_{\mathbf{x}} \partial_0 \langle \bar\chi \gamma_0\gamma_5 \tau^1 \chi(x) \bar\chi \gamma_5 \tau^1 \chi(0)\rangle}{a^3 \sum_{\mathbf{x}} \langle \bar\chi \gamma_5 \tau^1 \chi(x) \bar\chi \gamma_5 \tau^1 \chi(0)\rangle}\Big|_{\beta,\mu} = 0 \,, \tag{1.2}$$

at values of x_0 and L so large that the (charged) one-pion state dominates the correlators on the r.h.s. This prescription fixes the lattice artifact $O(a\Lambda_{QCD}^2)$ in the critical mass in such a way that, provided $\mu \gtrsim a^2\Lambda_{QCD}^3$, the dominating (relative) cutoff effects left-over in physical observables [2] are expected to be numerically as small as $O(a^2\Lambda_{QCD}^2)$. A detailed analysis [6] shows that such cutoff effects are actually products of (two) terms of order $a\Lambda_{QCD}$, $a\mu$ (negligible for small μ) or $a^3\Lambda_{QCD}^4\mu^{-1}$ (higher order in a, but enhanced for small μ).

In practice, as we are interested in simulations with $\mu \gtrsim \mu_{LOW}$, in order to minimise the work for the tuning of κ, we choose to impose the condition (1.2) only for $\mu = \mu_{LOW}$. With this choice, in the region where $\mu < \Lambda_{QCD}$ we expect [6, 1] the numerically dominating cutoff effects on physical observables to be modulated by factors of μ_{LOW}/μ as μ is varied (for instance one can have contributions from terms of order $(a\Lambda_{QCD}\mu_{LOW}/\mu)^2$). With κ fixed according to the criterion described above, maximal twist is implemented properly, provided

$$\mu \gtrsim \mu_{LOW} \geq C a^2 \Lambda_{QCD}^3 \,, \tag{1.3}$$

[1] Here quark bilinears are written in the unphysical quark basis (χ, $\bar\chi$) where the Wilson term has its standard form.

[2] Concerning the π^0-mass, in Ref. [7] it is argued that the possibly large $O(a^2)$ artifact on this observable is merely due to the large value taken by a (continuum) matrix element present in the Symanzik expansion of all lattice correlators where the π^0 state contributes, rather than to the presence of dimension six operators with large coefficients in the Symanzik effective action. This implies that this cutoff effect represents an exceptional, though important case.

where the coefficient C has to be learned from numerical experiment. In our $N_f = 2$ setup, $C \sim 2$ (assuming $\Lambda_{QCD} = 250$ MeV) is essentially determined by the condition that MC simulations exhibit no metastabilities (see e.g. Ref. [8], sect. 5.5). At fixed μ_R a smooth approach to the continuum limit is to be expected if maximal twist has been realized at (approximatively) the same value of $\mu_{R\,LOW}$ in physical units for all the considered lattice resolutions.

Our practical implementation of maximal twist is illustrated by Fig. 1a, where we show $m_R r_0 \propto m_{PCAC}$ vs. $\mu_R r_0 \propto \mu$ for $\beta = 4.05$, 3.9 and 3.8 (use of renormalized quantities eases the comparison). Details on r_0/a and Z_P (actually $Z_P(\overline{MS}, 2\,GeV)$) are given below.

For $\beta = 4.05$ and 3.9 we could fulfill our criterion for maximal twist at $\mu_{R\,LOW} \simeq 0.047 r_0^{-1}$ with good statistical precision: as shown in Fig. 1a, $m_R/\mu_{R\,LOW} = Z_A m_{PCAC}/\mu_{LOW}$ is consistent with zero within the statistical error, that we call ε/μ_{LOW}. As a rule of thumb, we demand ε/μ_{LOW} to be such that, numerically, $a\Lambda_{QCD}\varepsilon/\mu_{LOW} \lesssim 0.01$. Considering the form of the $d = 5$ term in the Symanzik effective Lagrangian one finds in fact that $a\Lambda_{QCD}\varepsilon/\mu$ is the expected order of magnitude of the unwanted (relative) cutoff effects that may contaminate physical observables if, due to numerical error, $m_{PCAC}(\beta, \mu)$ takes the value εZ_A^{-1}, rather than zero. Having no a priori control on the coefficients of this order of magnitude estimate, we can only learn from the numerical experience of a scaling test (involving our statistically most precise observables, *i.e.* f_{PS} and m_{PS}) whether our rule of thumb yields a sufficiently accurate tuning to maximal twist.

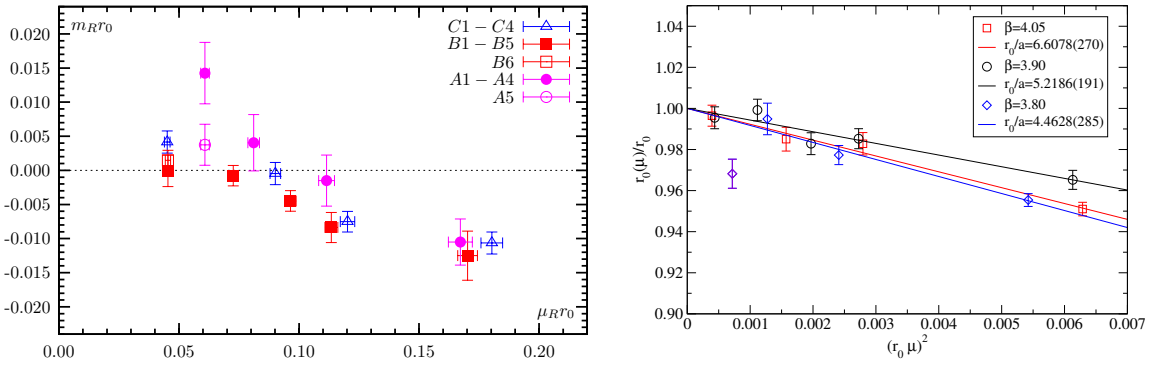

(a) (b)

Figure 1: (a) $m_R r_0 = Z_A Z_P^{-1} m_{PCAC} r_0$ vs. $\mu_R r_0$ and (b) $r_0(\mu)/r_0$ vs. $(\mu r_0)^2$, with $r_0 = \lim_{\mu \to 0} r_0(\mu)$ (see text). In both plots data for $\beta = 4.05$, 3.9, 3.8 and $L \simeq 2.1, 2.1, 2.4$ fm (respectively) are shown.

At $\beta = 3.8$ our implementation of maximal twist was not as precise as wished due to the long-range statistical fluctuations that, for $\mu_R \lesssim 0.1 r_0^{-1}$, were observed in our MC simulations (see Ref. [4] for information on autocorrelation times). These fluctuations, which increase in MC-time length and (weakly) in amplitude as μ decreases, have a major impact on those observables, such as the plaquette and am_{PCAC}, that are not continuous at the Singleton-Sharpe (1^{st} order) lattice phase transition [8, 9], rendering somewhat problematic the estimate of their statistical errors. This is manifest in Fig. 1a from the two non-coinciding points obtained for the lowest μ_R at $\beta = 3.8$, coming from two independent simulations at slightly different L (ensembles A1 and A5 in tab. 1 of Ref. [4]). In this case, the quoted (possibly underestimated) statistical errors are larger than

required by our rule of thumb.

1.2 Evaluation of r_0

In our scaling analyses we employ the Sommer scale r_0 [10] to eliminate the lattice spacing a. This is meant only as an intermediate step. In the end r_0 will be eliminated in favour of f_π (*i.e.* $f_{\rm PS}$ at the physical point) to get the scale for all dimensionful quantities. The value of r_0 for the various ensembles was obtained with a better than 0.5% accuracy, starting from Wilson loops made out of HYP-smeared temporal links [11] and APE-smeared spatial links. Employing several interpolating operators for static quark-antiquark ($Q\bar{Q}$) states, corresponding to different spatial smearings, leads to a matrix of correlators, from which the (lowest) levels of the potential $V_{Q\bar{Q}}(r)$ are estimated by solving a generalized eigenvalue problem. A fit to the r-dependence of the ground state gives $r_0(\mu)/a$. For each β, the latter shows a rather mild μ-dependence, which is well described by a first order polynomial in μ^2. The following values, extrapolated to the chiral limit and denoted simply as r_0/a, will be used in this work (those at $\beta = 4.05$ and $\beta = 3.8$ must be viewed as preliminary):

$$r_0/a|_{\beta=4.05} = 6.61(3)\,, \quad r_0/a|_{\beta=3.9} = 5.22(2)\,, \quad r_0/a|_{\beta=3.8} = 4.46(3)\,.$$

Note that a fit by a second order polynomial in μ gives compatible results. An overview of the results for $r_0(\mu)$ for all β's is given in Fig. 1b, where the axes are normalized in terms of the appropriate chirally extrapolated r_0. For $\beta = 3.8$ the point at the lowest μ-value (ensemble A1) is preliminary and carries a still poorly estimated statistical error. It was hence not used in the extrapolation to the chiral limit. More details will be given in a forthcoming publication.

2. Charged pion sector: general remarks

In the charged pseudoscalar (PS) meson sector our raw results for $f_{\rm PS}$ and $m^2_{\rm PS}$ from simulations at $\beta = 4.05$ and 3.9 with $L > 2$ fm, once expressed in units of r_0, exhibit an excellent scaling behaviour, see Fig. 4 of Ref. [4]. Also the corresponding results at $\beta = 3.8$, in spite of the uncertainties on the implementation of maximal twist and the estimate of statistical errors, appear consistent with a very good scaling behaviour in the mass range $m_{\rm PS} = (350 \div 600)$ MeV. These findings are in agreement with the expectation that cutoff effects are small in the absence of O(a) artifacts. In particular in the charged PS-meson sector it is known [5, 6] that, for small quark masses $\mu_{\rm R}$, $m^2_{\rm PS}$ differs from its continuum counterpart only by terms of O($a^2\mu_{\rm R}$) and O(a^4), while $f_{\rm PS}$ has discretization errors of O(a^2). This property holds for any volume L^3 (sufficiently large to make pions much lighter than other states) and is not affected by the lattice artifact on the neutral PS-meson mass. [3] In other words, to order a^2 the cutoff effects on $m^2_{\rm PS}$ and $f_{\rm PS}$ are like in a chirally invariant lattice formulation. The use of continuum chiral formulae to describe the volume and quark mass dependences of our data in the charged PS-meson sector is thus well justified.

2.1 Estimates of Z_P and of the renormalized quark mass

In the study of the scaling of the renormalized quark mass μ_R one needs the renormalization constant $Z_P(\beta; aq)$ at a common scale q for all the considered values of β. This renormalization

[3] The relation of a possibly large and negative lattice artifact on $m^2_{\pi^0}$ to metastabilities in MC simulations has been discussed in Refs. [1, 8]. Such metastabilities are not observed in the simulations we consider here [4].

constant, as well as the scale-independent one $Z_A(\beta)$, was also employed in Fig. 1a. [4] Preliminary O(a) improved estimates of the renormalization constants of quark bilinear operators are reported in Ref. [12]. There the results for Z_A are rather precise (at the 1.5% level), while the quoted uncertainties on Z_P are still substantially larger.

In view of this situation, in our scaling analysis of μ_R we do not use the values of Z_P quoted in Ref. [12]. We rather employ the scale- and scheme-independent ratios $Z_P(\beta;aq)/Z_P(\beta_{\rm ref};a_{\rm ref}q)$, which we extract with a statistical accuracy of $\sim 1\%$ from the relation (exact up to O(a^2) terms)

$$Z_P(\beta;aq)\,/\,Z_P(\beta_{\rm ref};a_{\rm ref}q) \;=\; \mu(\beta;m_{\rm PS}r_0=1;L/r_0\simeq 5)\,/\,\mu(\beta_{\rm ref};m_{\rm PS}r_0=1;L/r_0\simeq 5)\,, \quad (2.1)$$

in order to compare the values of $\mu_R(\beta;aq)Z_P(\beta_{\rm ref};a_{\rm ref}q)$ at different values of β and of the PS-meson mass. In eq. (2.1), $a\mu(\beta;m_{\rm PS}r_0=1;L/r_0\simeq 5)$ is the value of $a\mu$ for which, at a given β and $L/r_0\simeq 5$, one finds $m_{\rm PS}r_0=1$. [5] The scaling is obviously not affected by the extra overall factor $Z_P(\beta_{\rm ref};a_{\rm ref}q)$, which is removed in the end (in order to give an idea of the values of the renormalized quark masses). In the following we choose $\beta_{\rm ref}=3.9$, where we most reliably know (see Ref. [12]) $Z_P(\beta_{\rm ref};a_{\rm ref}q)$, we evaluate for $\beta=4.05$ and $\beta=3.8$ the Z_P-ratios from eq. (2.1) and we finally obtain estimates of $\mu_R(\beta;aq)$ at $q=2$ GeV in the $\overline{\rm MS}$ scheme for all β's. An important drawback of this method is the fact that cutoff effects stemming from data obtained at different β-values mix up in the quark mass renormalization, which in general may fake the genuine a-dependence and cast doubts on the reliability of any continuum extrapolation. Nevertheless, since our data for $\beta=4.05$ and 3.9 show no statistically significant cutoff effects in the relation of $f_{\rm PS}$ to $m^2_{\rm PS}$ and in the values of $\mu_R(\beta;aq)Z_P(\beta_{\rm ref};a_{\rm ref}q)$, we can obtain an estimate of the continuum limit of μ_R (in units of r_0) by taking an average of the results at these two β-values. A similar remark holds for the determination of $\widehat{B}_0$ and the chiral condensate in sect. 4. As discussed below, for all observables we associate to our continuum limit estimates a conservative systematic error obtained by comparing them to the corresponding results from data at $\beta=3.8$.

2.2 About taking the continuum, thermodynamical and chiral limits

It is well known that matching simulation data obtained at finite L and for $m_{\rm PS}\geq 300$ MeV to the physical pion point requires a delicate analysis. The impact of residual O(a^2) effects (even if small) on such an analysis might be enhanced if the continuum limit is performed as the last step. It is therefore advisable to perform first a continuum limit extrapolation at different (suitably chosen) fixed physical conditions and then use Chiral Perturbation Theory (χPT) to correct for finite size effects and reach the physical pion point. This is the strategy we follow in sect. 4.1.1, based on the results of the scaling test presented in sect. 3.1. As far as one is concerned with data, such as those at $\beta=4.05$ and 3.9, where no significant cutoff effects are observed, a conceptually equivalent approach is that of performing a combined analysis of all data by means of continuum χPT formulae. The outcome of this approach, which is detailed in Ref. [4], is summarised in sect. 4.1.2. For comparison we also discuss in sect. 4.1.3 the results of fits to continuum χPT formulae where the data corresponding to different lattice spacings are treated separately.

[4] For the renormalization constants we keep the names they are given in the literature for the standard (untwisted) Wilson quark lattice formulation, as obviously their values do not change with respect to the untwisted Wilson case.

[5] This value of $m_{\rm PS}r_0$ was chosen so as to lie in the region where errors from interpolation to the reference mass and cutoff effects are smallest.

3. Charged pion sector: scaling test

Here we analyse the scaling behaviour of the charged PS-meson decay constant and the renormalized quark mass as $a \to 0$ at fixed values of $m_{\rm PS} r_0$ and L/r_0. The renormalization and scaling conditions are as follows: (i) $r_0^2 F_{Q\bar{Q}}(r_0) = 1.65$ (with $F_{Q\bar{Q}}$ the static interquark force), which allows to trade $g_0^2 = 6/\beta$ with r_0/a ; (ii) $m_{\rm PS} r_0 =$ constant $\in \{0.7, 0.8, 0.9, 1.0, 1.1, 1.25\}$, which eliminates μ in favour of $m_{\rm PS}$; (iii) fixed spatial volume $L^3_{\rm ref} \simeq (2.2 \text{ fm})^3$, which corresponds to $L/r_0 \simeq 5$.

3.1 Scaling and preliminary continuum limit estimates

The typical relative statistical errors are (conservatively) estimated to be about 0.7% for $m_{\rm PS} r_0$, 1.0% for $f_{\rm PS} r_0$ and 1.5% for $\mu_{\rm R} r_0$. In the latter case, besides the error on r_0/a, only the uncertainty (typically about 1.2%) on the Z_P-ratios (see eq. (2.1)), is taken into account and hence shown in Fig. 3. The error on $Z_P(\beta_{\rm ref}; a_{\rm ref} q)$ is omitted here, as it plays no role, while in sect. 4 it is taken into account, as it matters for the final values of $\widehat{B}_0$, the chiral condensate and m_{ud}.

The condition (i) is immediately fulfilled once all quantities are expressed in units of r_0. As for the other two conditions, we first implement the condition (iii) by "moving" via resummed χPT formulae (see Ref. [14]) the data for $f_{\rm PS}$ and $m_{\rm PS}$ from the simulation volume L^3 to the reference one $L^3_{\rm ref}$. As simulations were done with $L \in (2.0, 2.4)$ fm, the numerical change in the data is very tiny (never larger than 0.7%) and thus statistically almost irrelevant. Then, in order to match the reference values of $m_{\rm PS} r_0$ given in (ii), we perform interpolations (in few cases also short extrapolations) of the values of $f_{\rm PS} r_0$ and μr_0. For this purpose we try both (low order) polynomial and χPT-inspired fits to the data. The spread among the different fits with good χ^2, whenever statistically significant, is added linearly to the interpolation error. In this way one ends up with the blue filled circle data points (and errorbars) in the Figs. 2 and 3.

For each value of $m_{\rm PS} r_0$ we obtain preliminary estimates of the continuum limit values of $f_{\rm PS} r_0$ and $\mu_{\rm R} r_0$ by fitting to a constant (red line in the figures) *only* the data points from simulations at $\beta = 4.05$ and $\beta = 3.9$. The results, with only statistical error from the continuum extrapolation, are shown in red in Figs. 2 and 3. In all cases the difference between the result of the continuum extrapolation and the central value (blue filled circle point) for $\beta = 3.8$ is taken as an estimate of the systematic error (indicated with a green cross placed at a slightly negative value of a) on the continuum limit result. Since the latter is obtained by simply taking a weighted average of the results at $\beta = 4.05$ and 3.9, the introduction of such an error appears necessary. Moreover, the quality of the data in the figures suggests that the way we estimate this systematic error is rather conservative. Finally, the green crosses (and errorbars) appearing in Figs. 2 and 3 at $(a/r_0)^2 \sim 0.05$ show, whenever the displacement is larger than one standard deviation, where the actual data would move if one were correcting for the leading effect of the numerical error (denoted by ε in sect. 1.1) in imposing $m_{\rm PCAC} = 0$. We refer to the results of such a correction (explained in sect. 3.2) as to "data moved to maximal twist".

3.2 About "moving data to maximal twist"

The procedure of "moving data to maximal twist" can be seen as a way of testing whether statistical errors in the tuning to maximal twist have any significant impact on the observables of interest. If one has $Z_A m_{\rm PCAC} = \varepsilon$ (rather than zero), the effective twist angle in the Symanzik

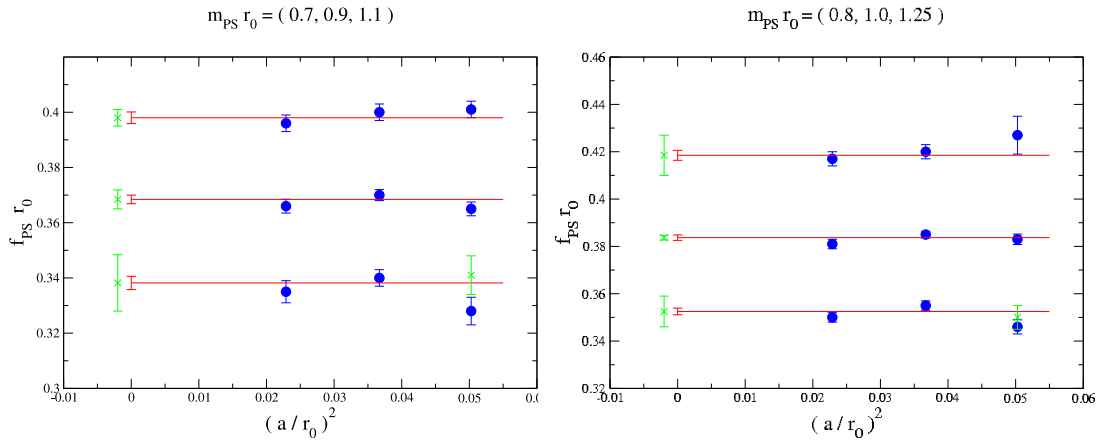

(a) (b)

Figure 2: Scaling plots of $f_{\rm PS} r_0$ vs. $(a/r_0)^2$ at fixed values of $m_{\rm PS} r_0$ (increasing from bottom to top). See text for a detailed explanation of the symbols.

Lagrangian is $\alpha = \pi/2 - \theta$ with $\tan\theta = m_R/\mu_R = \varepsilon/\mu$. Treating ε as an $O(a^0)$ quantity and neglecting $O(a\theta)$ and $O(a^2)$ effects, the consequences of a deviation from maximal twist are in general twofold. First, the effective renormalized quark mass becomes $M_R = (\mu_R^2 + m_R^2)^{1/2} = \mu_R/cos\theta$. Second, in all operator matrix elements any operator formally non-invariant under axial-τ^3 transformations must be reinterpreted consistently with the twist angle being $\alpha = \pi/2 - \theta$ (rather than $\pi/2$). As a consequence, once the hadronic states of interest are correctly identified, simple θ-dependent formulae can be derived that allow to extract properly the matrix elements of operators non-invariant under axial-τ^3 transformations. For instance, the (renormalized) operator $Z_V \bar\chi \gamma_\mu \tau^2 \chi$ (written in the basis where the Wilson term has its standard form) coincides with $\cos\theta A^1_{\mu\, R} + \sin\theta V^2_{\mu\, R}$, where $A^1_{\mu\, R}$ ($V^2_{\mu\, R}$) is the physical axial (vector) current. Consequently one finds $< \pi^1 | Z_V \bar\chi \gamma_\mu \tau^2 \chi | \Omega > |_{m_R,\mu_R} = \cos\theta < \pi^1 | A^1_{\mu\, R} | \Omega > |_{M_R} + O(a\theta, a^2)$, which implies $m_{\rm PS} f_{\rm PS}|_{M_R} = < \pi^1 | Z_V \bar\chi \gamma_0 \tau^2 \chi | \Omega > |_{m_R,\mu_R} / \cos\theta + O(a\theta, a^2)$.

From these arguments it follows that $m_{\rm PS}$-data need not be moved, while the data for $\mu_{\rm R}$ and $f_{\rm PS}$ are "moved to maximal twist", up to $O(a\theta, a^2)$, by dividing them by $\cos\theta$, where θ is obtained from the (interpolated) actual values of ε and μ in our data sets. It turns out that the change implied by this correction is larger than one standard deviation (of the uncorrected data) only for the two smallest reference values of $m_{\rm PS} r_0$ at $\beta = 3.8$. After such correction all the data points at $\beta = 3.8$ (including the two most chiral ones) fit very nicely into the scaling picture suggested from the corresponding data at $\beta = 3.9$ and $\beta = 4.05$.

However, any data where the above correction was statistically relevant can be hardly used for a continuum extrapolation, because the residual (uncorrected) $O(a\theta)$ lattice artifacts depend on the details of the numerical errors at the different β-values and hence need not to scale as $a \to 0$. Nevertheless, at a more qualitative level, the procedure of "moving data to maximal twist" confirms that, even at $\beta = 3.8$ (*i.e.* $a \simeq 0.1$ fm), the lattice artifacts in the charged PS-meson sector appear to be quite small, provided maximal twist is implemented precisely, e.g. according to the criteria

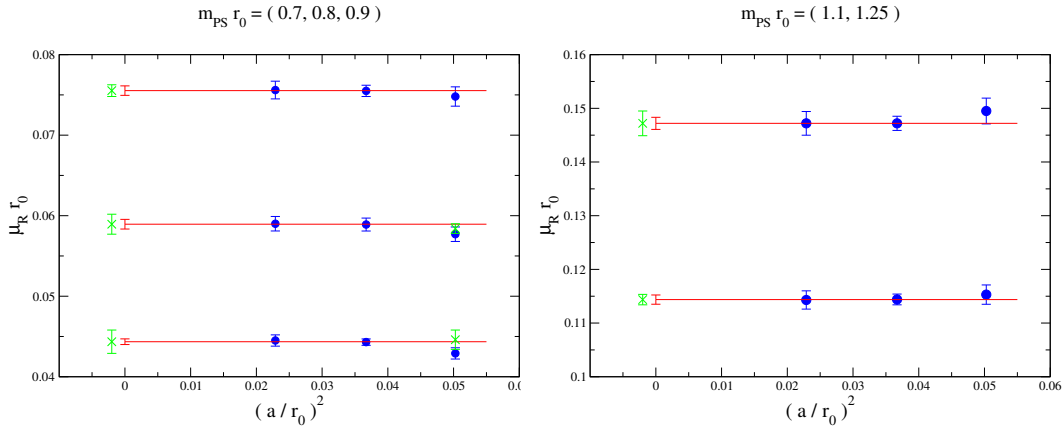

(a) (b)

Figure 3: Scaling plot of $\mu_R r_0$ vs. $(a/r_0)^2$ at fixed values of $m_{PS} r_0$ (increasing from bottom to top). See text for a detailed explanation of the symbols.

of sect. 1.1. In fact such a precise implementation is rather hard to achieve in the case of our simulations at $\beta = 3.8$, as we found $\tau_{int}(am_{PCAC}) = O(100)$, see sect. 1.1 and Ref. [4].

4. Charged pion sector: physical results

Here we discuss the description of our m_{PS}- and f_{PS}-data by means of *continuum* χPT for $N_f = 2$ QCD and give preliminary estimates of the low energy constants (LEC) $\bar{l}_3$, $\bar{l}_4$, $\widehat{B}_0$ and f_0,[6] as well as of the average light quark mass, m_{ud}, and the chiral condensate.

We employ the following continuum NLO χPT formulae [13, 14] to simultaneously describe the dependence of m_{PS} and f_{PS} on the bare quark mass (μ) and on the finite spatial size (L):

$$m^2_{PS}(L) = 2B_0\mu\, K^2_m(L)\, \left[1 + \xi \ln(2B_0\mu/\Lambda^2_3)\right] , \tag{4.1}$$

$$f_{PS}(L) = f_0 K_f(L)\, \left[1 - 2\xi \ln(2B_0\mu/\Lambda^2_4)\right] , \tag{4.2}$$

where $\xi = 2B_0\mu/(4\pi f_0)^2$ and $K_{m,f}(L)$ account for finite size (FS) effects. The LEC $\bar{l}_{3,4}$ are related to the parameters $\Lambda_{3,4}$ introduced in eqs. (4.1)–(4.2) through $\bar{l}_{3,4} \equiv \log(\Lambda^2_{3,4}/m^2_{\pi^\pm})$. The expressions for $K_{m,f}(L)$ at NLO (denoted as GL) read [13]: $K^{GL}_m(L) = 1 + \frac{1}{2}\xi\tilde{g}_1(\lambda)$ and $K^{GL}_f(L) = 1 - 2\xi\tilde{g}_1(\lambda)$, where $\lambda = \sqrt{2B_0\mu L^2}$ and $\tilde{g}_1(\lambda)$ is a known function. A convenient way to include higher order χPT terms in the description of FS effects on m_{PS} and f_{PS} is provided by the formulae of Ref. [14] (denoted by CDH). In the following we always use the CDH expressions for $K_{m,f}(L)$, which turn out [4] to describe well our data at different volumes (and for m_{PS} better than GL formulae).

In all the analyses below physical units are introduced as follows: the experimental values, $f_\pi = 130.7$ MeV and $m_{\pi^0} = 135.0$ MeV,[7] are exploited to determine first the μ-value, μ_π, cor-

[6] We use the convention $f_0 = \sqrt{2}F_0$, *i.e.* the normalization $f_\pi = 130.7$ MeV.

[7] The π^0-mass input is chosen in view of the absence of electromagnetic effects in our lattice QCD simulations.

responding to the "physical point" through $m_{PS}/f_{PS}|_{\mu_\pi} = m_{\pi^0}/f_\pi$, and then (depending on the analysis) the value of $r_0 f_\pi$, or $a f_\pi$. The latter allows to express all quantities in units of f_π.

4.1 Chiral fits and continuum estimates of LEC

As anticipated in sect. 2.2, given the good scaling behaviour of our data, we present *preliminary* continuum estimates of LEC and m_{ud} that stem from two analyses – see sects. 4.1.1 and 4.1.2. In sect. 4.1.3 we give the corresponding results that are obtained at two fixed lattice spacings, $a(\beta = 4.05)$ and $a(\beta = 3.9)$. The latter results will serve mainly for estimating (in the way detailed below) the systematic error due to residual $O(a^2)$ cutoff effects.

Concerning other systematic errors, we note: (i) residual uncertainties in the CDH-formulae for FS effects are small, compared to other systematic errors – see the discussion in Ref. [4]; (ii) the possible impact of NNLO corrections to the formulae (4.1)–(4.2) for the quark mass dependence is minimized by taking out of the analyses the points with highest values of m_{PS} (we checked that fits are stable if we leave out data with $m_{PS} > 500$ MeV – more details in a forthcoming publication).

4.1.1 χPT fits in the continuum

Following the strategy presented in sect. 2.2 one can estimate the continuum limit values of $f_{PS}r_0$ and $\mu_R r_0$ at fixed values of $m_{PS}r_0$ and L_{ref}/r_0, as reported in sect. 3.1. Considering $f_{PS}r_0$ and $m_{PS}r_0$ as functions of $\mu_R r_0$ allows for direct use of the χPT formulae (4.1)–(4.2) to bring our data from $L_{ref} = 2.2$ fm to infinite volume and parameterise their quark mass dependence. Leaving out the point corresponding to $m_{PS}r_0 = 1.25$, the data are well described by our fit ansatz and we obtain the following values for the fit parameters:

$$\begin{aligned} 2\widehat{B}_0 r_0 &= 12.0(3)(7), \qquad \bar{l}_3 = 3.67(12)(35), \\ f_0 r_0 &= 0.266(3)(10), \qquad \bar{l}_4 = 4.69(4)(11), \end{aligned} \tag{4.3}$$

where the renormalized quantity $\widehat{B}_0 = Z_P B_0$ is given in the $\overline{\text{MS}}$-scheme at the scale $q = 2$ GeV (see sect. 2.1). The χ^2/dof of the fit is 0.28. Using the experimental input at the physical pion point we find $r_0 = 0.433(5)(16)$ fm. Inserting the values of r_0/a (see sect. 1.2), one gets the estimates

$$a|_{\beta=4.05} = 0.0655(8)(24) \text{ fm}, \quad a|_{\beta=3.9} = 0.0830(10)(31) \text{ fm}, \quad a|_{\beta=3.8} = 0.0970(13)(37) \text{ fm}.$$

In the above results, except for the case of $2\widehat{B}_0 r_0$, the second error comes entirely from the systematic uncertainty due to residual $O(a^2)$ cutoff effects: for each quantity this error is conservatively taken as the maximum of (i) the uncertainty resulting from the propagation through the chiral analysis of the systematic error associated to the continuum estimates as derived in sect. 3.1 and (ii) the spread of the results obtained separately at $\beta = 3.9$ and $\beta = 4.05$ (by fitting to the same χPT ansatz as here – see sect. 4.1.3). In practice the maximum is usually given by the former of these two systematic error estimates. Note however that for $\widehat{B}_0$, m_{ud} and the chiral condensate, an additional systematic uncertainty coming from Z_P (as quoted in Ref. [12]) is added in quadrature.

As a check, we also study the decay constant f_{PS} as a function of m_{PS}, *i.e.* with no reference to μ_R. The appropriate NLO χPT fit ansatz is obtained (ignoring NNLO corrections) by replacing $2B_0\mu$ with m_{PS}^2 in eq. (4.2). The resulting best fit parameters are $f_0 r_0 = 0.268(3)(12)$ and $\bar{l}_4 = 4.82(4)(14)$. This is consistent with the values in eq. (4.3) and yields for the Sommer scale

	single-β fit	single-β fit	combined fit – see sect. 4.1.2	
β	3.9	4.05	3.9	4.05
$2aB_0$	4.85(4)	3.87(6)	4.87(4)	3.76(3)
af_0	0.0526(4)	0.0404(7)	0.0527(4)	0.0411(4)
Λ_3/f_0	6.36(26)	7.20(48)	6.41(26)	
Λ_4/f_0	11.59(19)	11.81(31)	11.51(21)	
χ^2/dof	7.8/6	2.2/4	12.0/12	
$a\mu_\pi$	0.00072(2)	0.00054(2)	0.00072(1)	0.00057(1)
a [fm]	0.0854(6)	0.0656(10)	0.0855(5)(31)	0.0667(5)(24)

Table 1: Results from χPT fits at single β-values and from the global combined fit of sect. 4.1.2.

the estimate $r_0 = 0.435(4)(15)$ fm. The second error again comes from (the propagation of) the systematic uncertainty in the "continuum extrapolation" of sect. 3.1.

4.1.2 χPT analysis combining $\beta = 3.9$ and 4.05

As argued in sect. 2.2, given the absence of statistically relevant cutoff effects, one can combine the data (in lattice units) for $m_{\rm PS}$ and $f_{\rm PS}$ coming from our simulations at $\beta = 3.9$ and $\beta = 4.05$ and perform a global combined fit based again on eqs. (4.1)–(4.2). Such a combined fit has six free parameters which can be taken as $(aB_0)|_{\beta=3.9}$, $(aB_0)|_{\beta=4.05}$, $(af_0)|_{\beta=3.9}$, $(af_0)|_{\beta=4.05}$, Λ_3/f_0 and Λ_4/f_0. Details and plots concerning this analysis can be found in Ref. [4]. The outcome is summarised in table 1.[8] As for the estimates of a, the second error we quote is an estimate (see sect. 4.1.1) of the systematic uncertainty due to residual cutoff effects. We note that, leaving out the cases for which $m_{\rm PS} > 500$ MeV, nine ensembles of gauge configurations enter this analysis: five at $\beta = 3.9$ (B_1 to B_4 and B_6) and four at $\beta = 4.05$ (C_1 to C_3 and C_5).

4.1.3 Independent χPT analyses at $\beta = 3.9$ and 4.05 and comparison

These analyses, always based on eqs. (4.1)–(4.2), are closely analogous to that presented in Ref. [1]. The free parameters can be taken to be aB_0, af_0, Λ_3/f_0 and Λ_4/f_0, the best fit values of which are given in table 1 and illustrated in Fig. 4. For the case of $\beta = 3.9$ the only difference with respect to Ref. [1] is the increased statistics and in particular the presence of the ensemble B_6. For both $\beta = 4.05$ and $\beta = 3.9$ the same ensembles are considered as in the case of the global combined fit of sect. 4.1.2. It should be noted that in the analysis of sect. 4.1.1 the ensembles C_5 and B_6 were not employed, in order to avoid to heavily rely on the CDH-formulae in the "continuum extrapolations" discussed in sect. 3.1. On the other hand using these two ensembles, in particular B_6 (which corresponds to $L \sim 2.7$ fm) increases the statistical information.

In table 2 results from the independent analyses at $\beta = 3.9$ and 4.05, the combined fit of sect. 4.1.2 and the fit in the continuum of sect. 4.1.1 are compared (the second error, whenever quoted, is the systematic one previously discussed). The agreement between the last two columns

[8] From this analysis, without using r_0, we find $a|_{\beta=3.9}/a|_{\beta=4.05} = 1.28(1)$, which is quite close to $(r_0/a)|_{\beta=4.05}/(r_0/a)|_{\beta=3.9} = 1.27(1)$. Moreover, the comparison of the ratios $f_0/B_0|_{\beta=3.9}$ and $f_0/B_0|_{\beta=4.05}$ provides a rather precise estimate of the ratio $Z_P(\beta = 3.9; a_{\beta=3.9}q)/Z_P(\beta = 4.05; a_{\beta=4.05}q)$.

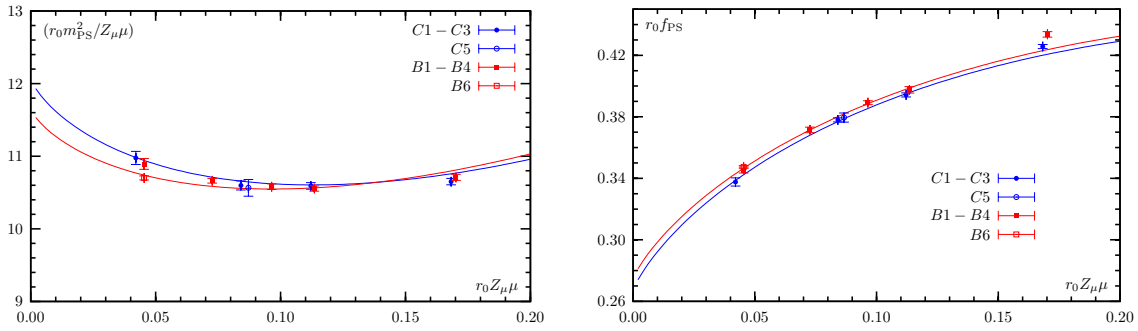

(a) (b)

Figure 4: Independent χPT fits at $\beta = 4.05$ and $\beta = 3.9$: FS-corrected data à la CDH for (a) $r_0 m_{PS}^2/\mu_R$ and (b) $r_0 f_{PS}$ vs. $\mu_R r_0$ are shown, with the corresponding best fit curves to eqs. (4.1)–(4.2). The points at $\mu_R r_0 \sim 0.17$ were not included in the fit.

	single-fit at $\beta = 3.9$	single-fit at $\beta = 4.05$	combined fit	fit in the continuum
$\bar{l}_3$	3.41(9)	3.66(14)	3.44(8)(35)	3.67(12)(35)
$\bar{l}_4$	4.62(4)	4.66(7)	4.61(4)(11)	4.69(4)(11)
$2r_0\widehat{B}_0$	11.6(3)(5)	11.9(3)(5) ÷ 12.1(3)(5)	11.6(3)(7)	12.0(3)(7)
$f_0 r_0$	0.275(2)	0.267(5)	0.273(3)(10)	0.266(3)(10)
r_0 [fm]	0.446(4)	0.434(7)	0.444(4)(16)	0.433(5)(16)

Table 2: Estimates of LEC and r_0 from the analyses of sects. 4.1.3 (1st and 2nd column), 4.1.2 (3rd column) and 4.1.1 (last column). The values of $2r_0\widehat{B}_0$ are obtained using Z_P at $\beta = 3.9$ [12] and Z_P-ratios from the analyses of sects. 4.1.2 and 4.1.1: at $\beta = 4.05$ we quote the two (similar) results obtained in this way.

of table 2 is good, even within statistical errors only. We recall that the ensembles B_6 and C_5 do not contribute to the results in the last column. Were these ensembles not used also in the combined fit of sect. 4.1.2, the results in the third column of table 2 would get, as expected, even closer to those in the last column: $\bar{l}_3 = 3.66(9)$, $\bar{l}_4 = 4.64(5)$, $2r_0\widehat{B}_0 = 11.9(3)$, $f_0 r_0 = 0.270(3)$, $r_0 = 0.439(5)$ fm. For reviews on determinations of the LEC we refer to Refs. [15, 16].

4.2 Continuum estimates of m_{ud} and the chiral condensate

Our preliminary results in the $\overline{\rm MS}$-scheme at scale $q = 2$ GeV are obtained using the RI-MOM estimate [12] of Z_P at $\beta = 3.9$ (converted to $\overline{\rm MS}$ by using NNNLO perturbation theory) and the Z_P-ratios from the analysis of sect. 4.1.2 (combined fit) or 4.1.1 (fit in the continuum). The average light quark mass $m_{ud}(\overline{\rm MS}, 2{\rm GeV})$ from the fit in the continuum reads $m_{ud} = 3.43(9)(23)\,{\rm MeV}$. From the combined fit we get $m_{ud} = 3.62(10)(23)$ MeV (using all the ensembles) and $m_{ud} = 3.49(13)(23)$ MeV (when excluding ensembles B_6 and C_5, *i.e.* with the same set of ensembles as for the fit in the continuum). When considering data at $\beta = 3.9$ *only* (as in sect. 4.1.3), we obtain $m_{ud} = 3.62(13)(23)$ MeV. This value is compatible with the one coming from the partially quenched analysis of Ref. [17], $m_{ud} = 3.85(12)(40)\,{\rm MeV}$.

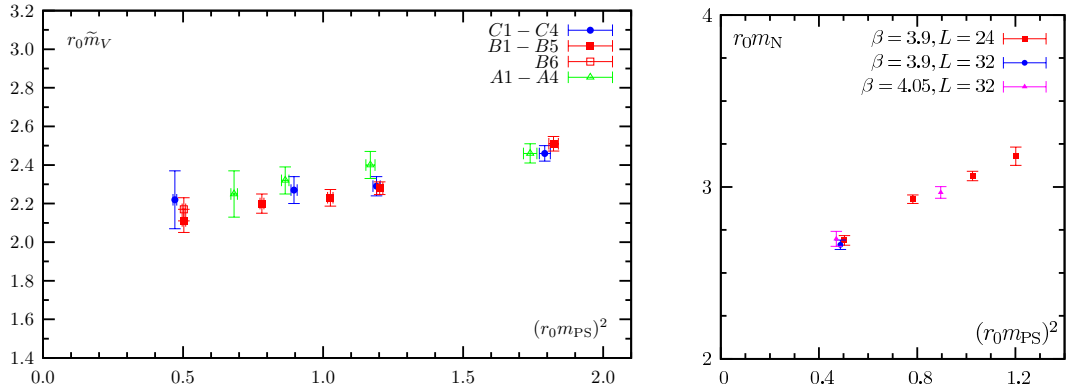

Figure 5: $\widetilde{m}_V r_0$ and $m_N r_0$ vs. $(m_{PS} r_0)^2$ for different lattice resolutions and L in the range $2.1 \div 2.4$ fm.

The chiral quark condensate is obtained through $\langle\bar{q}q\rangle(\overline{\rm MS}, 2{\rm GeV}) = -(1/2) f_0^2 \widehat{B}_0(\overline{\rm MS}, 2{\rm GeV})$. From the fit after the continuum extrapolation we get $|\langle\bar{q}q\rangle|^{1/3} = 272(4)(7)\,{\rm MeV}$, while from the combined fit analysis we obtain $|\langle\bar{q}q\rangle|^{1/3} = 267(4)(7)\,{\rm MeV}$ (and $|\langle\bar{q}q\rangle|^{1/3} = 270(4)(7)\,{\rm MeV}$ when the ensembles B_6 and C_5 are not used). These results are in agreement with an independent estimate at $\beta = 3.9$ from the ε regime – see Ref. [18].

5. Scaling analysis of other hadronic observables

Here we briefly report on the scaling behaviour of other hadronic observables. Even if at $\beta = 3.8$ preliminary data are available only for the meson vector mass and the physical volumes at the various lattice resolutions ($L \simeq 2.1$ fm for $\beta = 4.05, 3.9$ and $L \simeq 2.4$ fm for $\beta = 3.8$) are only approximatively matched, this overview suggests that when employing maximally twisted Wilson quarks the cutoff effects on physical quantities are in general as small as expected on the basis of O(a) improvement.

5.1 Nucleon and vector meson masses

In Fig. 5, we show our data (in units of r_0) for the vector meson "mass", $\widetilde{m}_V$, and the nucleon mass, m_N, as a function of m_{PS}^2. For the former one (see Ref. [19] for more details), the scaling appears to be good, although within statistical errors that become of few percents when $m_{PS} \sim 300 \div 350$ MeV. In this case, we remark that what we call the "mass" may differ from the actual vector meson mass (the one that becomes m_ρ as $m_{PS} \to m_\pi$), owing to the effect of virtual ρ–$\pi\pi$ mixing. [9] Due to the finite volume, the decay of the ρ-meson (at rest) into real $\pi\pi$ states is instead forbidden, even when $2m_{PS} < m_V$ (which roughly speaking happens in the region $(m_{PS} r_0)^2 \lesssim 1$). The data for the nucleon mass are also preliminary (see Ref. [20]): at $\beta = 4.05$ only two data points are available, which however appear to agree quite well with the data points at $\beta = 3.9$.

[9] The correction is estimated [19] to be almost irrelevant within our present statistical errors: at our most chiral point, where $m_{PS} \sim 300$ MeV, it amounts to $\widetilde{m}_V - m_V \sim 0.05 m_V$.

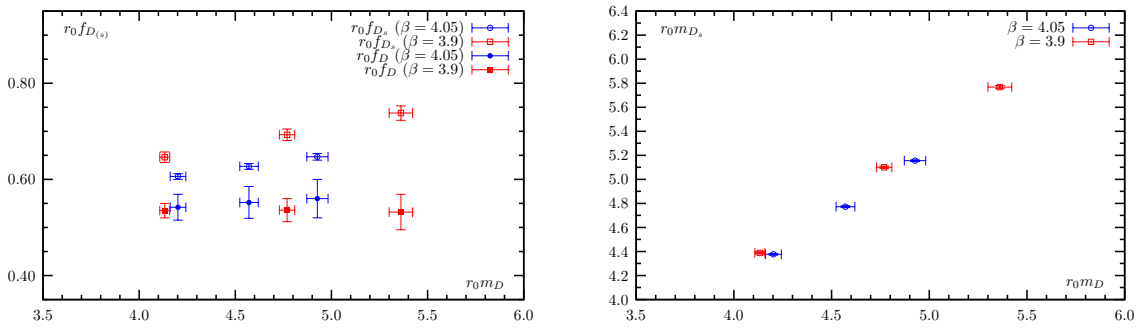

(a) (b)

Figure 6: $f_D r_0$, $f_{D_s} r_0$ (a) and $m_{D_s} r_0$ (b) vs. $m_D r_0$ for two lattice spacings ($\beta = 4.05$ and 3.9) and $L \sim 2.1$ fm.

5.2 Charmed observables in partially quenched setup

To compute charmed observables we adopt a partially quenched (PQ) setup, which is detailed in Ref. [21]. [10] With the notation of Ref. [22] for valence quarks, the correlators for D ($\bar{c}d$) and D_s ($\bar{c}s$) charged mesons are computed with Wilson parameters $r_d = r_s = -r_c = 1$, in order to have the same nice parametric scaling properties as in the charged pion sector. For the present considerations about scaling we choose close-to-realistic renormalization conditions: $m_{PS} r_0 = 0.7092$ and $\mu_{\tilde{s}}/\mu_{\tilde{c}} = 0.082$ (instead of the realistic conditions $m_\pi r_0 \simeq 0.30$ and $\mu_s/\mu_c \simeq 0.088$). In Figs. 6, m_D varies with $\mu_{\tilde{c}}$ at fixed values of $\mu_{\tilde{s}}/\mu_{\tilde{c}}$ and $m_{PS} r_0$ (*i.e.* μ_{ud}). The expected size of the dominating cutoff effects is $(a\mu_{\tilde{c}})^2 \sim 0.1$, since typically, $a\mu_{\tilde{s}} \in [0.020, 0.033]$ and $a\mu_{\tilde{c}} \in [0.25, 0.40]$. By comparing the preliminary results from $\beta = 4.05$ and $\beta = 3.9$, we see that the observed scaling violations are not large: from 1–2% (hardly visible within statistical errors) for f_D and m_{D_s} to 7–8% for f_{D_s}. Data from a third lattice spacing, $\beta = 3.8$, are currently being analysed and may allow for an estimate of continuum limit results.

6. Conclusions and outlook

We have reported on the scaling properties of lattice QCD with $N_f = 2$ maximally twisted Wilson quarks, in the unitary [4] as well as in a partially quenched setup [17, 21]. Very good scaling properties are found in the light (charged) PS-meson sector and also for various charmed PS-meson observables, as well as in the vector meson and the parity-even nucleon channels, in agreement with the expectation of automatic O(a) improvement of physical observables. Based on these findings, we presented χPT-based analyses suggesting that the determinations of the LEC's (among which those relevant for the chiral condensate) and of the average u,d quark mass that were obtained for one single lattice resolution in Refs. [1, 17] are likely to be close to their continuum limit $N_f = 2$ QCD values. Moreover, combining the results presented here with those of Ref. [20],

[10] The proof of automatic O(a) improvement given in Ref. [22] for a fully unquenched mixed action framework goes through also in the PQ mixed action setup of Ref. [21], where the quark masses of the valence s and c quarks are taken finite and hence different from those (infinite in the present case) of the corresponding sea quarks.

after appropriate chiral extrapolations, one finds an estimate of the ratio m_N/f_π that is in good agreement with experiment. The framework of lattice QCD with maximally twisted Wilson quarks appears thus to offer good prospects for reliable computations of many physical QCD observables and weak matrix elements in the continuum limit.

Acknowledgements

We thank all our ETM collaborators for many important contributions to this work. In particular we are grateful to those who directly provided us with specific results: C. Alexandrou (nucleon mass), B. Blossier (charmed observables – besides a crucial contribution to the computation of r_0 at $\beta = 3.8$), C. Michael (vector meson mass), V. Lubicz and S. Simula (renormalization constants). This work was partially supported by the EU Contract MRTN-CT-2006-035482 "FLAVIAnet".

References

[1] ETM Collaboration, Ph. Boucaud *et al.*, Phys. Lett. **B650**, 304 (2007), [hep-lat/0701012].

[2] C. Urbach, K. Jansen, A. Shindler and U. Wenger, Comput. Phys. Commun. **174**, 87 (2006), [hep-lat/0506011].

[3] R. Frezzotti and G.C. Rossi, JHEP **0408**, 007 (2004), [hep-lat/0306014].

[4] ETM Collaboration, C. Urbach, PoS(LATTICE 2007)022 [arXiv:0710.1517].

[5] S.R. Sharpe and J.M.S. Wu, Phys. Rev. **D71** (2005) 074501, [hep-lat/0411021].

[6] R. Frezzotti, G. Martinelli, M. Papinutto and G.C. Rossi, JHEP **0604** 038 (2006), [hep-lat/0503034].

[7] ETM Collaboration, R. Frezzotti and G.C. Rossi, PoS(LATTICE 2007)277.

[8] A. Shindler, arXiv:0707.4093 [hep-lat].

[9] S. R. Sharpe, Phys. Rev. D **72** (2005) 074510, [hep-lat/0509009].

[10] R. Sommer, Nucl. Phys. B **411** (1994) 839 [arXiv:hep-lat/9310022].

[11] M. Della Morte, A. Shindler and R. Sommer, JHEP **0508** (2005) 051, [hep-lat/0506008].

[12] ETM Collaboration, P. Dimopoulos *et al.*, PoS(LATTICE 2007)241 [arXiv:0710.0975].

[13] J. Gasser and H. Leutwyler, Phys. Lett. **B184**, 83 (1987).

[14] G. Colangelo, S. Dürr and C. Haefeli, Nucl. Phys. **B721**, 136 (2005), [hep-lat/0503014].

[15] H. Leutwyler, arXiv:0706.3138 [hep-ph].

[16] S. Necco, PoS(LATTICE 2007)021.

[17] ETM Collaboration, B. Blossier *et al.*, [arXiv:0709.4574];
C. Tarantino *et al.*, PoS(LATTICE 2007)374 [arXiv:0710.0329].

[18] ETM Collaboration, A. Shindler *et al.*, PoS(LATTICE 2007)084.

[19] ETM Collaboration, C. Michael and C. Urbach, PoS(LATTICE 2007)122 [arXiv:0709.4564].

[20] ETM Collaboration, C. Alexandrou *et al.*, PoS(LATTICE 2007)087 [arXiv:0710.1173].

[21] ETM Collaboration, B. Blossier *et al.*, PoS(LATTICE 2007)346 [arXiv:0710.1414].

[22] R. Frezzotti and G.C. Rossi, JHEP **0410** (2004) 070, [hep-lat/0407002].